

Fig. 2-5-2 Geological Map with Section Lines of the Camarones Area

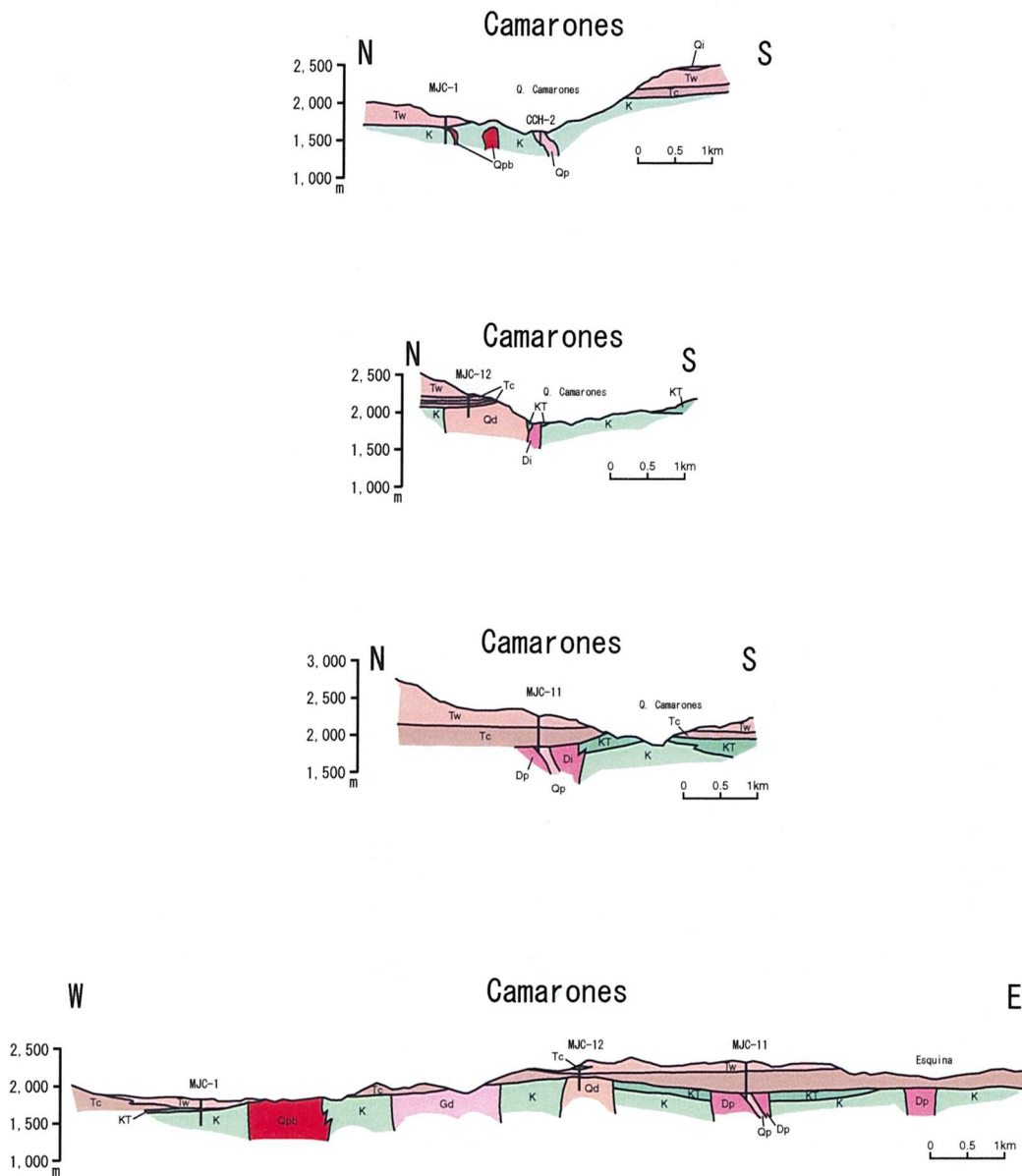


Fig.2-5-3 Geological Profiles of the Camarones Area

537

(5) Minimiñe area (MJC-9)

A geological map of the area is shown in Figure 2-2-71 and geological cross section in Figure 2-2-72.

MJC-9:

① Geology

The geology of this hole consists of, from bottom upward, Miocene-Pliocene ignimbrite, Upper Neogene-Quaternary conglomerate and ignimbrite, and Pleistocene-Holocene gravel and talus deposits.

The Miocene-Pliocene ignimbrite is pink to gray, and consists of quartz-biotite-bearing rhyolitic welded tuff with intercalation of thin crystalline tuff beds.

The Upper Neogene-Quaternary conglomerate is dark gray to brown, and consists of andesitic~dacitic pebbles with in intercalation of crystalline tuff and pumiceous tuff beds in the upper part.

The Upper Neogene-quaternary ignimbrite is pink to brown, and consists of quartz-biotite-rich rhyolitic welded tuff.

The Pleistocene-Holocene gravel and talus deposits consist of andesitic~dacitic pebbles, crystalline tuff and pumiceous tuff blocks.

② Alteration~mineralization

Notable alteration and mineralization are not found in this hole, only sericitization is partly observed below 484m depth.

(6) Area to the northeast of Camiña area (MJC-10)

A geological map of the area is shown in Figure 2-2-67 and geological cross section in Figure 2-2-68.

MJC-10:

① Geology

The geology of this area consists of Upper Neogene-Quaternary basalt lava and alluvium.

The basalt lava is dark gray and aphyric. Strongly altered rocks are intercalated in various places.

The alluvium is thinly distributed over a wide area consisting of pebbles and sand.

② Alteration-mineralization

Strong argillization consisting of kaolin-smectite is widely developed in this hole, and is partly silicified.

Limonite dissemination occurs in 14~24m depth interval, and fine-pyrite dissemination below 36m depth. Cu-As-Hg anomalies are observed in the alteration zone in 14~36m and 68~82m depth intervals (Fig. 2-5-4).

5 - 3 Magnetic Anomalies and Geology and Mineralization

Of the 12 holes drilled in the overlap zones of intermediate airborne magnetic intensity zones and the peripheries of the medium wavelength anomaly zones, three (MJC-1, 11, 12) in Camarones area reached the porphyry-copper horizon of pre-Early Oligocene formation (pre-Lower Oligocene Series). MJC-1 and MJC-12 caught brecciated intrusive body and intrusive igneous body which are of the same nature as the igneous rocks related to porphyry copper mineralization, namely quartz porphyry. Also strong pyrite mineralization was confirmed in these holes. At MJC-12, quartz diorite believed to be of Eocene activity was confirmed and weak pyrite mineralization was confirmed.

On the other hand, the nine holes in areas other than Camarones, were drilled through Oligocene-Miocene conglomerate or younger formations. Of these, MJC-8 of Arica and MJC-2 of Codpa were drilled through Oligocene-Miocene conglomerate and approached pre-Oligocene units.

From geology of the holes and the magnetic susceptibility of the cuttings, regular relation between the basement depth and the airborne medium wavelength anomalies or short wavelength anomalies could not be found. In Camarones, the reason for reaching the pre-Lower Oligocene units was the short distance – less than 1km – from the pre-Lower Oligocene area on the surface.

The general trend of the variation of magnetic susceptibility of the cuttings can be correlated

to the geology and alteration of the drill holes. Namely, it is stronger in mafic igneous rocks, and that of the Tertiary and Neogene-Quaternary conglomerate is higher than that of pyroclastic rocks and shallow gravel beds. Also the magnetic susceptibility is relatively low in phyllic alteration zones, acidic alteration zones and oxidized zones while it is higher in propylitic alteration zones.

It is believed that the possibility of reaching porphyry-copper type mineralized-altered zones in the two drill holes of Camarones area, and the drill hole in Northeast of Camiña area (MJC-10) reached epithermal type mineralization alteration zone in Tertiary-Quaternary igneous bodies. It is believed to be possible that magnetic anomalies are closely related to igneous bodies and alteration, but as the number of drill holes reaching pre-Lower Oligocene units are small, it is not possible at this stage to confirm the relation between magnetic anomalies and porphyry-copper type mineralization and alteration. Also since mineralization is not observed in MJC-6 and 7 which have relatively similar geologic environment to MJC-10, there must be other factors controlling epithermal type mineralization and alteration other than the above magnetic anomalies (intermediate magnetic intensity zone and peripheries of the medium wavelength anomaly zones).

Table 2-5-2 Assay Results of Alteration Zones and Mineralization Zone

Zone	Hole No.	Depth (m)	Cu (ppm)	Mo (ppm)	Pb (ppm)	Zn (ppm)	S (%)		Pb/Cu
Oxi. Z.	MJC-1	136-142	37	6	25	42	0.84		0.66
Ser. Z.	MJC-1	142-184	45	6	8	45	4.52		0.08
Ser.-Chl. Z.	MJC-1	184-220	34	5	14	108	4.02		0.39
Chl.>Ser. Z.	MJC-1	220-266	31	5	6	94	3.02		0.22
Ser-Chl Z.	MJC-1	266-348	97	5	8	72	4.38		0.27
Oxi. Z.	MJC-11	428-456	26	6	35	35	0.37		1.45
Ser. Z.	MJC-11	456-500	20	7	14	102	1.83		0.82

Zone	Hole No.	Depth (m)	Cu (ppm)	Mo (ppm)	Pb (ppm)	Zn (ppm)	As (ppm)	Hg (ppm)	Pb/Cu
Acid A. Z.	MJC-5	178-186	8	5	30	10	237	0.028	4.02
Acid A. Z.	MJC-6	90-94	16	10	63	18	586	0.030	3.84
Acid A. Z.	MJC-6	124-146	17	4	18	34	245	0.017	1.12
Fresh z.	MJC-10	6-14	121	9	5	165	38	0.593	0.04
Oxi. Z.	MJC-10	14-24	192	7	5	121	343	1.881	0.03
Acid A. Z.	MJC-10	24-36	155	5	4	153	50	0.585	0.03
Fresh Z.	MJC-10	36-58	75	5	4	124	116	0.902	0.05
Acid A. Z.	MJC-10	58-82	167	4	8	51	406	3.115	0.08
Fresh Z.	MJC-10	82-120	68	5	7	85	24	0.233	0.10
Acid A. Z.	MJC-10	120-220	41	4	4	71	291	0.364	0.15
Fresh Z.	MJC-10	220-308	21	4	6	79	32	0.093	0.28
Acid A. Z.	MJC-10	308-342	22	2	6	74	24	0.154	0.31
Fresh Z.	MJC-10	342-350	46	3	1	81	23	0.073	0.03
Acid. A. Z.	MJC-10	350-372	52	2	6	70	24	0.274	0.12
Fresh Z.	MJC-10	372-384	62	5	10	89	105	0.331	0.16
Acid. A. Z.	MJC-10	384-394	52	2	10	82	177	0.122	0.20
Prop. Z.	MJC-12	164-300	111	5	8	88	4	0.006	0.08

abbrev.: Oxi. Z.=oxidized zone A.Z.=alteration zone Ser-Chl. Z.=sericitic-chloritic alteration zone
 Prop. Z.=propylitic alteration zone
 r=correlation coefficient

MJC - 1A

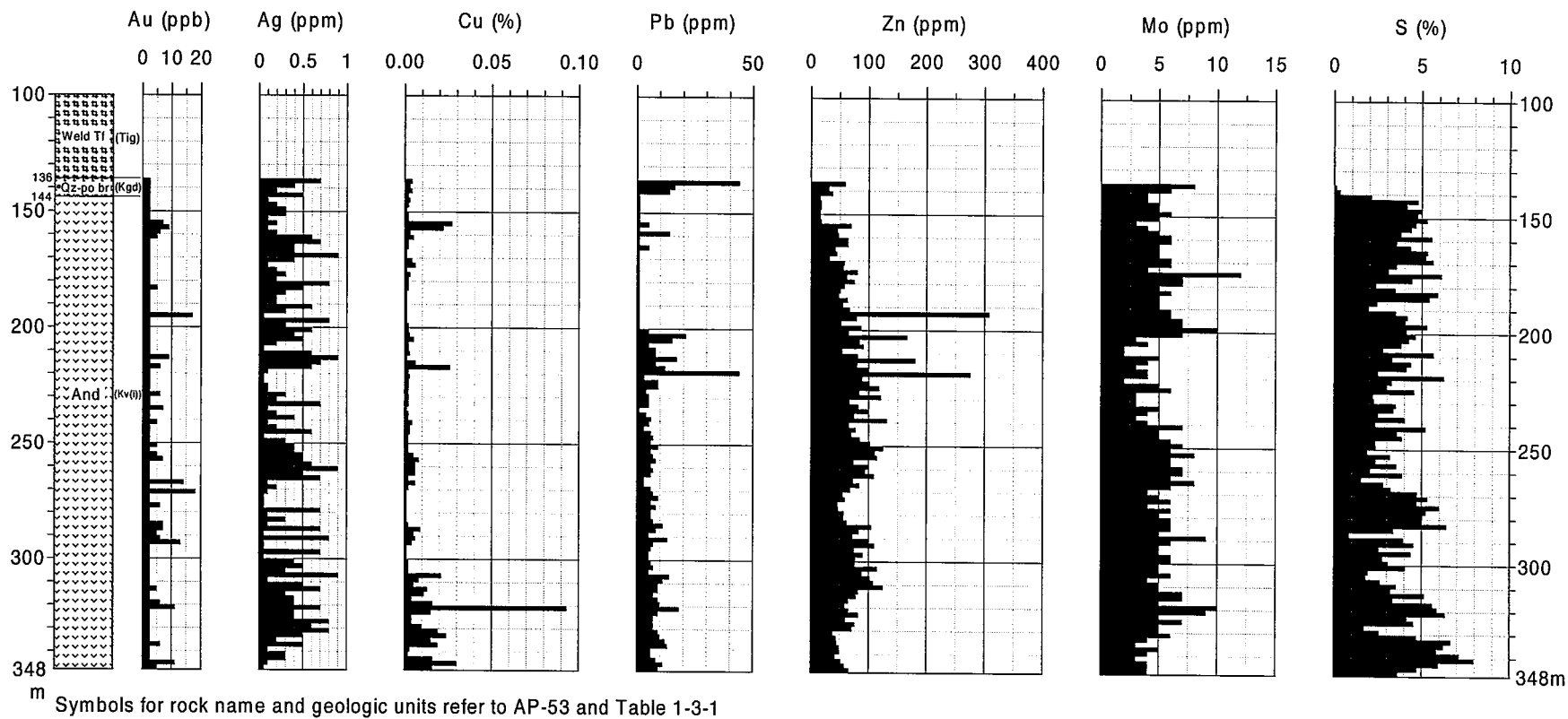


Fig. 2-5-4 Histogram of Assay Results of Drill Holes (MJC-1A)

543

MJC - 10

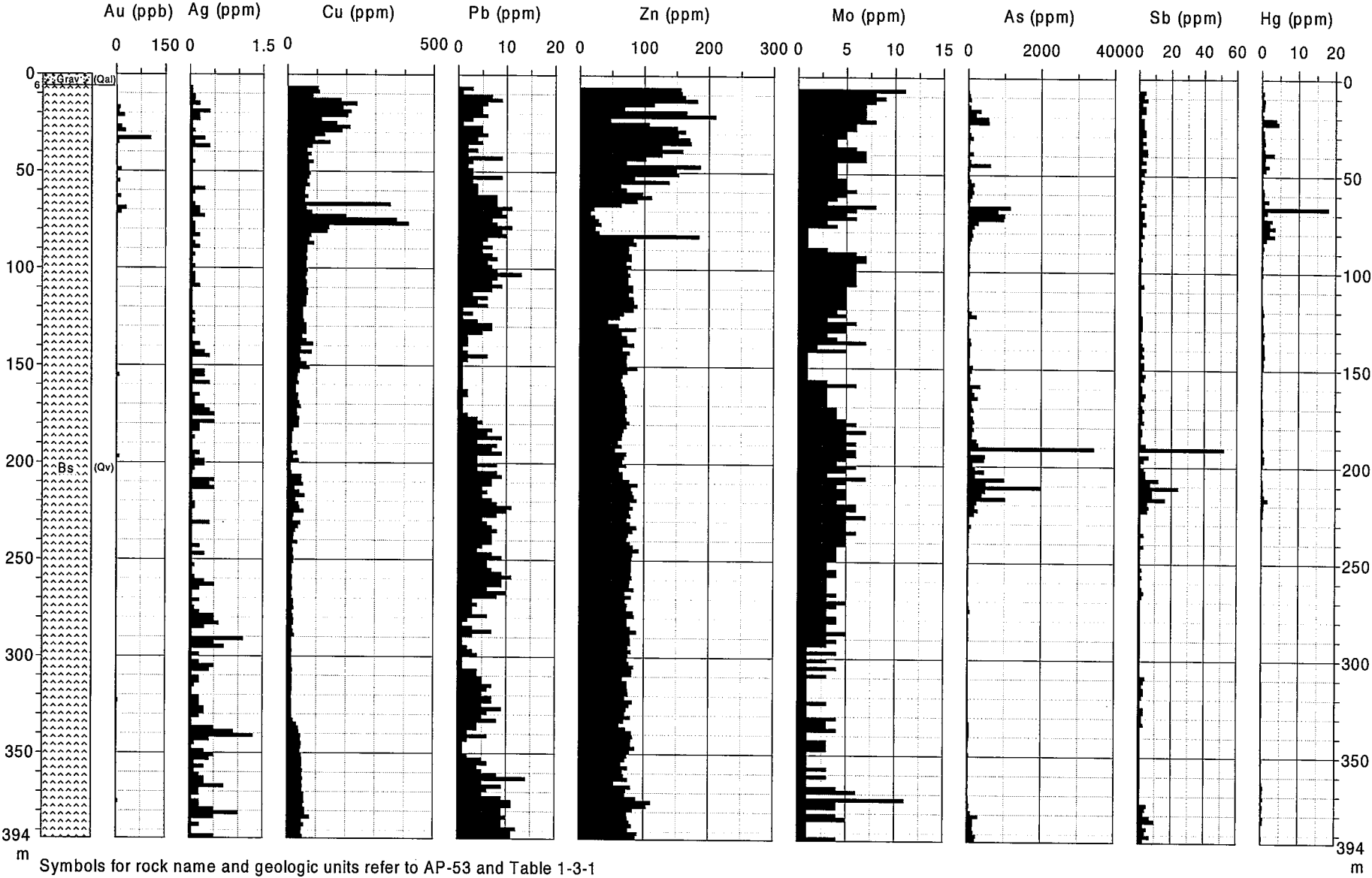
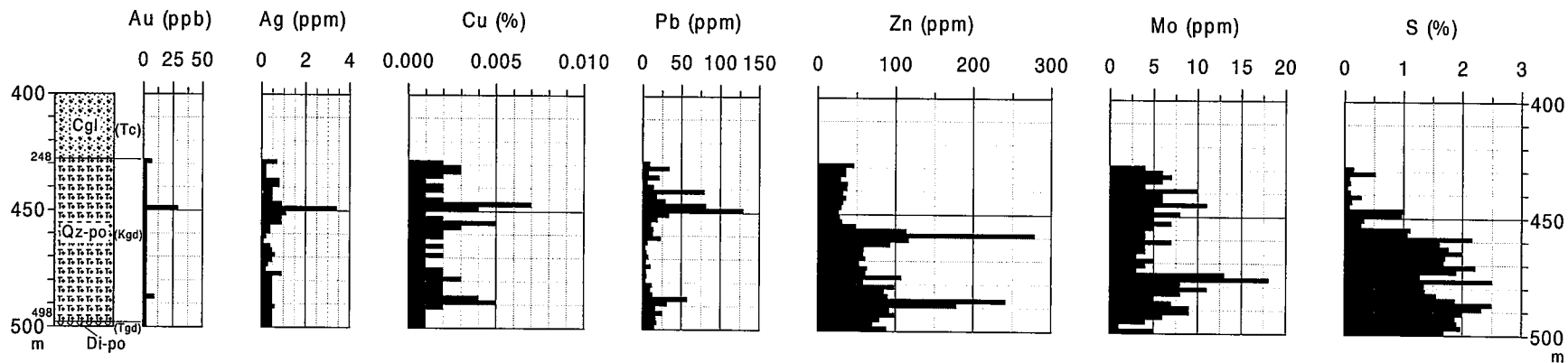


Fig. 2-5-4 Histogram of Assay Results of Drill Holes (MJC-10)

MJC - 11



MJC - 12

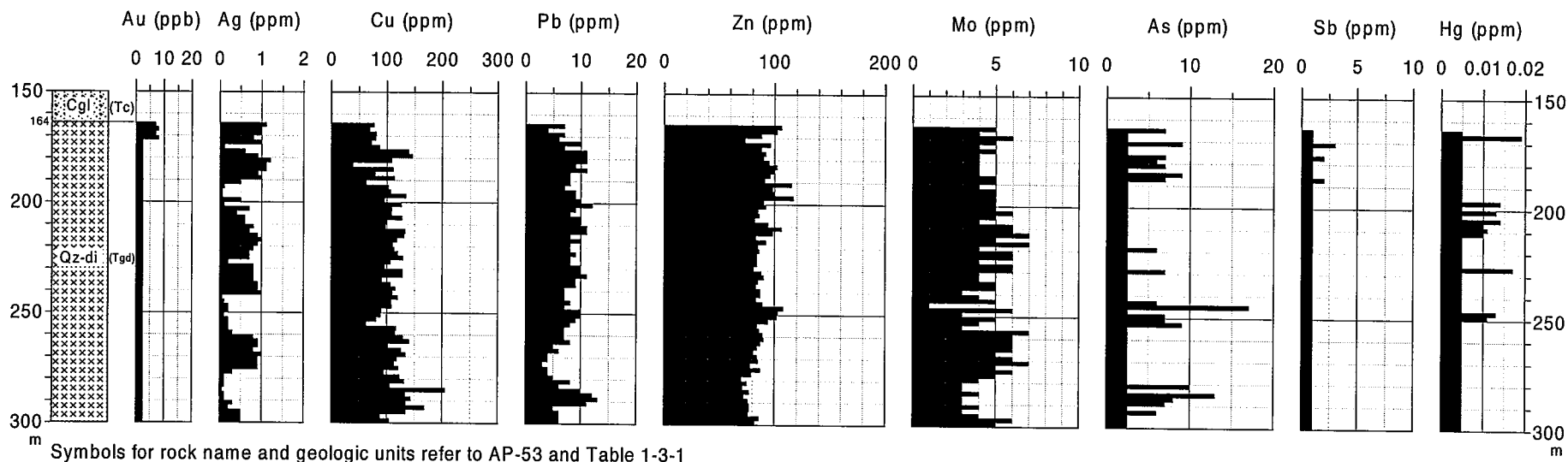


Fig. 2-5-4 Histogram of Assay Results of Drill Holes (MJC-11, MJC-12)

CHAPTER 6 RE-ANALYSIS OF AIRBORNE MAGNETIC DATA

6-1 Outline of Work

CODELCO has shown that high macroscopic correlation exists between the major porphyry copper deposits of northern Chile and transverse magnetic anomalies. This fully applies to the major porphyry copper deposits in the central to southern parts of Region I. But transverse magnetic anomalies are not clear in the northern part (See Figure 2-6) , and thus in the present survey investigation was not to limited to transverse magnetic anomalies, but all magnetic anomalies were analyzed and examined. Frequency analysis was adopted in order to consider the relation between porphyry copper deposits and magnetic anomalies in the level of individual anomalies.

A flowchart of the re-analysis work of the airborne magnetic data is laid out in Figure 2-6-1. Data acquisition, compilation of existing data, preparation of magnetic maps, magnetic structure analysis, and preliminary two-dimensional modeling were carried out during the second year of this project. Thus during the third year, magnetic susceptibility and remanent magnetism were measured for the entire Region I area, many magnetic anomalies were extracted by frequency analysis, and the results were evaluated for porphyry copper exploration.

The total magnetic intensity (TMI) map used for the analysis is shown in Figure 2-6-2. A magnetic map (RTP map) prepared by reducing TMI to the pole is shown in Figure 2-6-3. This map was used for the analyses and interpretations except two-dimensional modeling.

6-2 Results of Re-analysis

6-2-1 Separation of magnetic anomalies

RTP map shows magnetic anomalies formed by overlapping anomalies of various sizes. Frequency analysis was carried out with the purpose of separating these anomalies in order to distinguish them as independent magnetic anomalies. First, 6 kinds of RTP maps were prepared by extracting magnetic anomalies larger than; 4km, 7km, 12km, 17km, 24km, and 33km by high-cut filters. Then 4 kinds of RTP maps were prepared by extracting anomalies with sizes; 4~7km, 4~12km, 12~24km, and 12~33km by band-pass filters.

The magnetic anomalies which appear on these 10 maps and the location of the 26 known porphyry copper type mineralized zones were examined. The results indicated a close relation between the porphyry copper type mineralized zones and the 12~24km-size magnetic anomalies. The following three kinds of RTP maps were prepared on the basis of this result.

- short wavelength RTP map: anomalies over 12km were removed

- medium wavelength RTP map: anomalies over 24km and under 12km were removed
- long wavelength RTP map: anomalies under 24km were removed

These maps are laid out in Figures 2-6-4 to 2-6-6.

Next, each magnetic anomaly was distinguished and extracted from the above three RTP maps. Anomalies with RTP value of more than 60 ~ 80nT at the center of anomaly were extracted.

For short wavelength and medium wavelength magnetic anomalies, each extracted anomaly was sequentially numbered, and the coordinates, intensity, geologic information of the locality, access, and other relevant information were recorded in a inventory of SW/MW magnetic anomaly respectively. As for the long wavelength anomalies, they were only sequentially numbered.

The inventories of magnetic anomaly were prepared before the surface survey, and their geological and access information was useful for the selection of the sites for magnetic susceptibility measurements for the entire Region I area.

Overlay maps of short, medium, and long wavelength magnetic anomaly distribution, reduced to the pole magnetism and porphyry copper mineralized zones are laid out in Figures 2-6-7 to 2-6-9. It is seen from Figure 2-6-8 that, with the exception of the 4 localities west of Putre, 22 known porphyry copper mineralized zones out of 26 localities lie within or in the vicinity of medium wavelength anomalies.

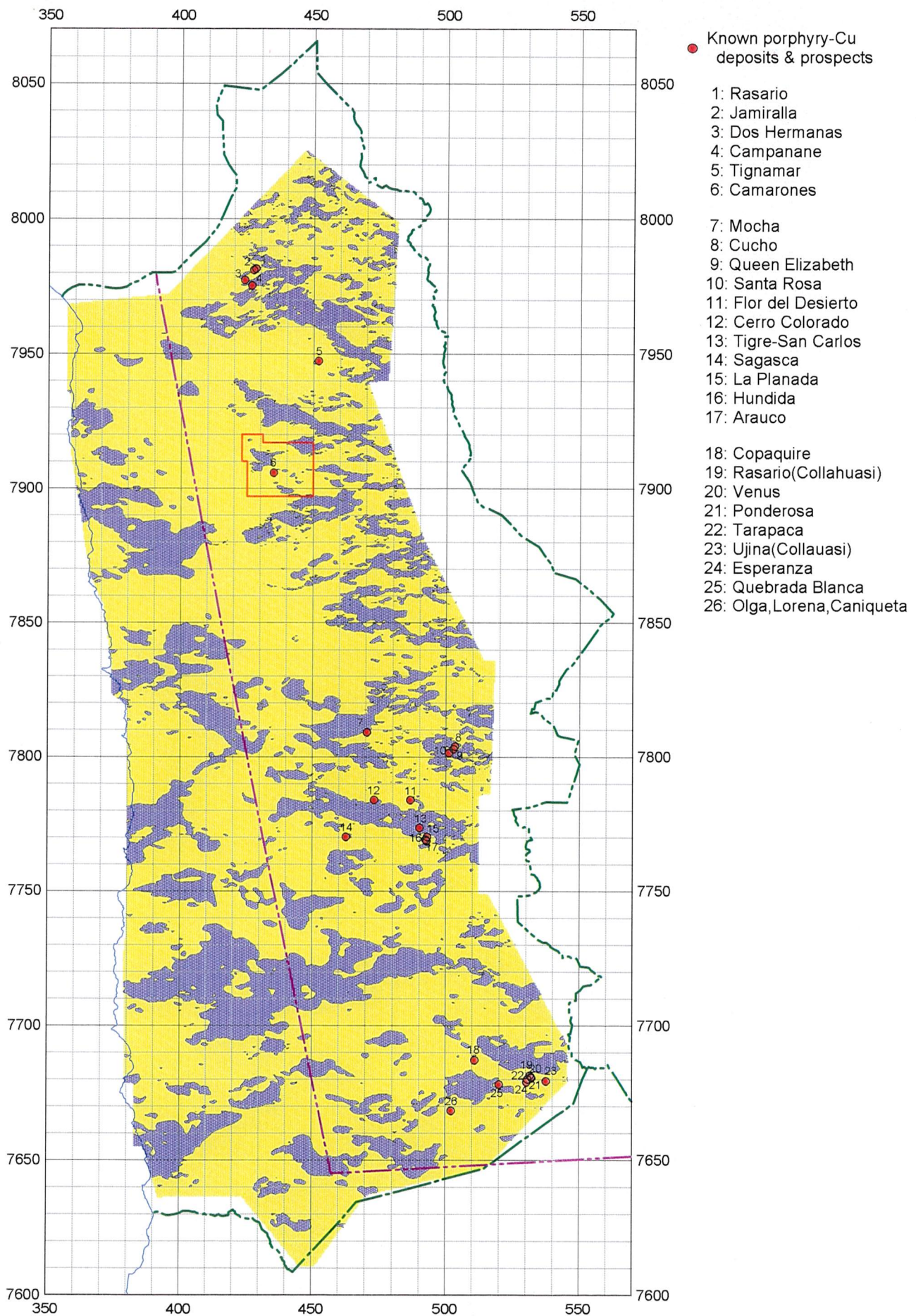


Fig. 2-6 Transverse Magnetic Anomalies and Known Porphyry-Cu Deposits & Prospects

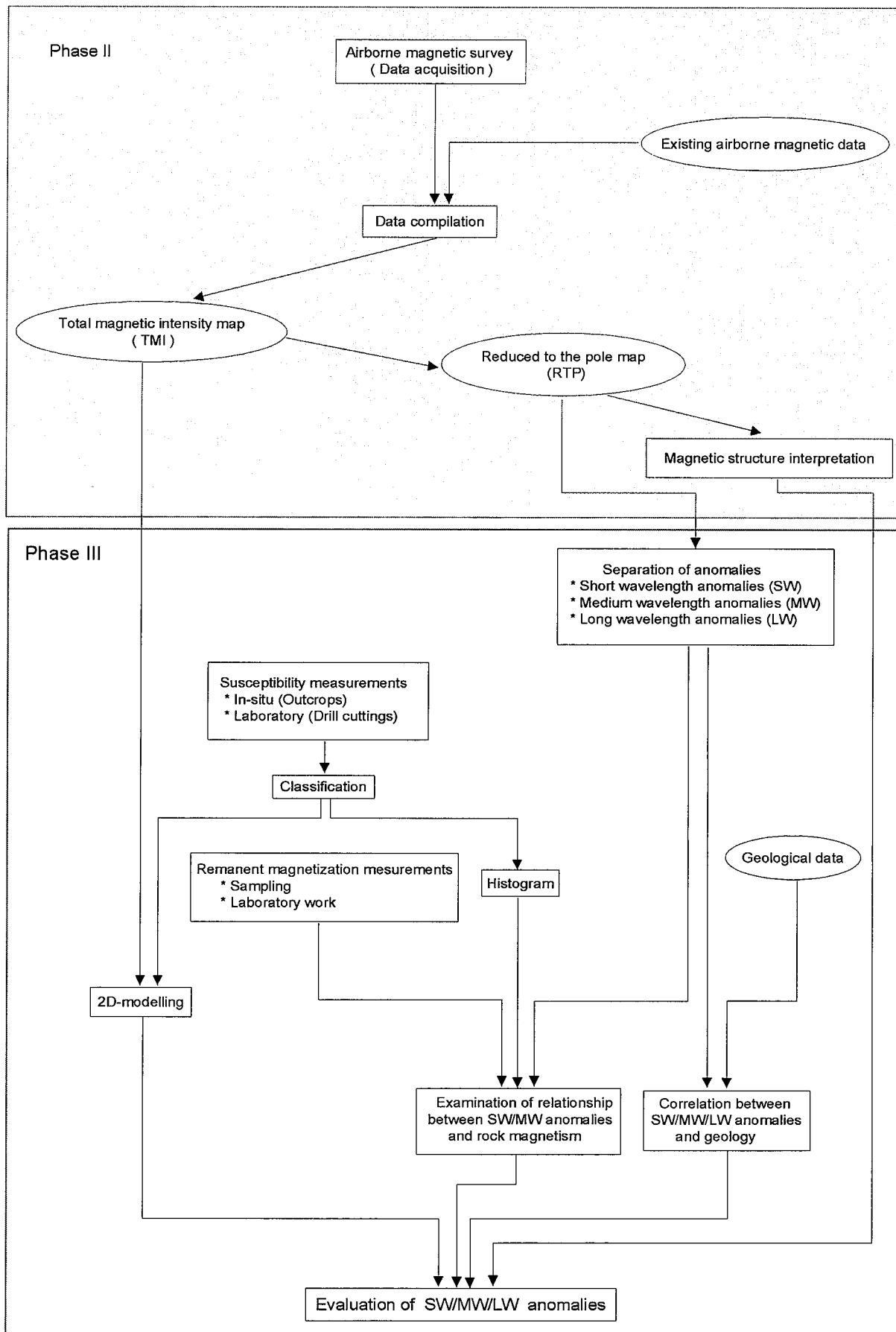


Fig. 2-6-1 Flowchart of Airborne Magnetic Interpretation

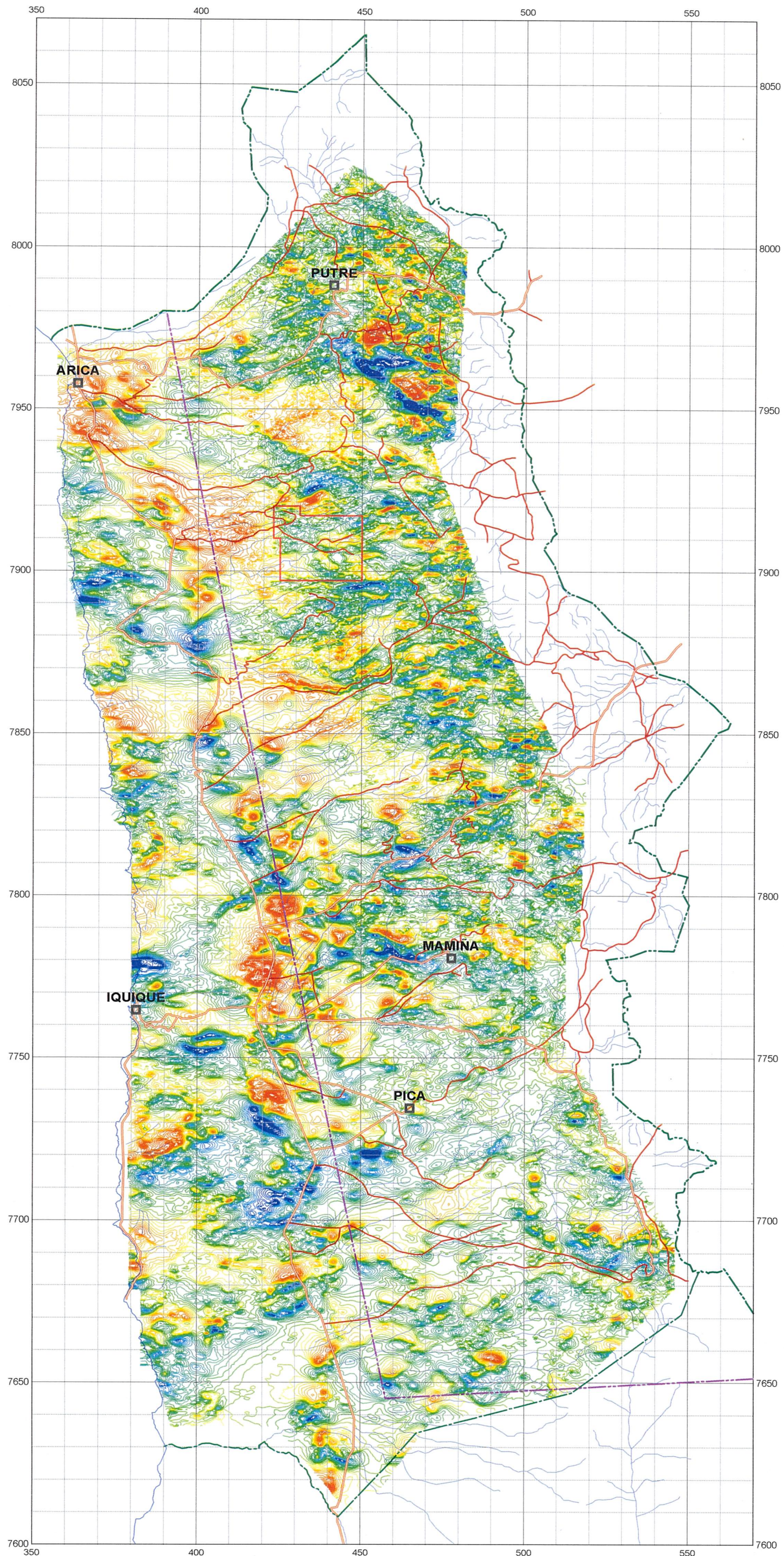


Fig.2-6-2
Total Magnetic Intensity Map

— 553 ~ 554 —

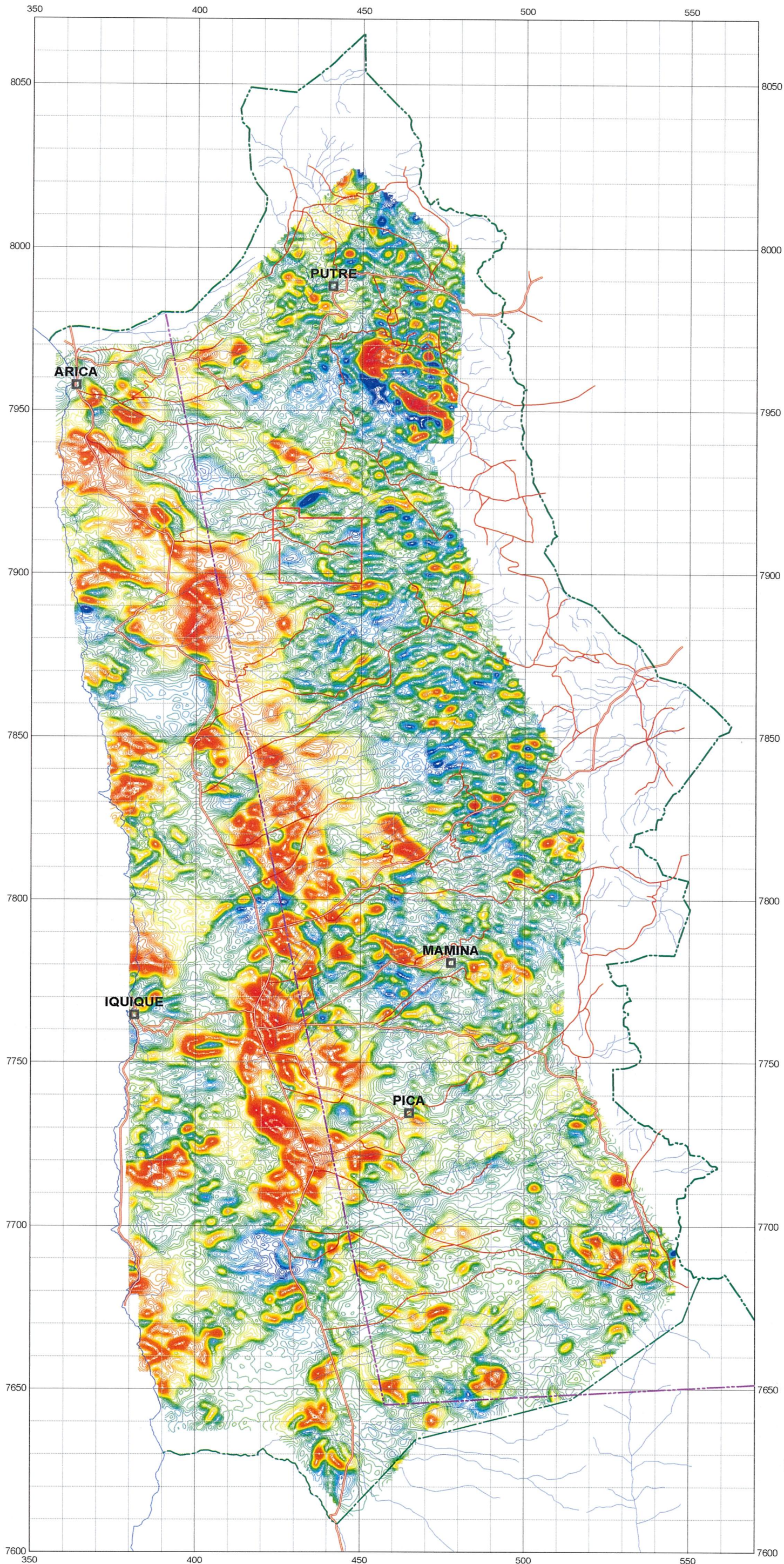


Fig.2-6-3
Reduced to the Pole Map



— 555 —
— 556 —

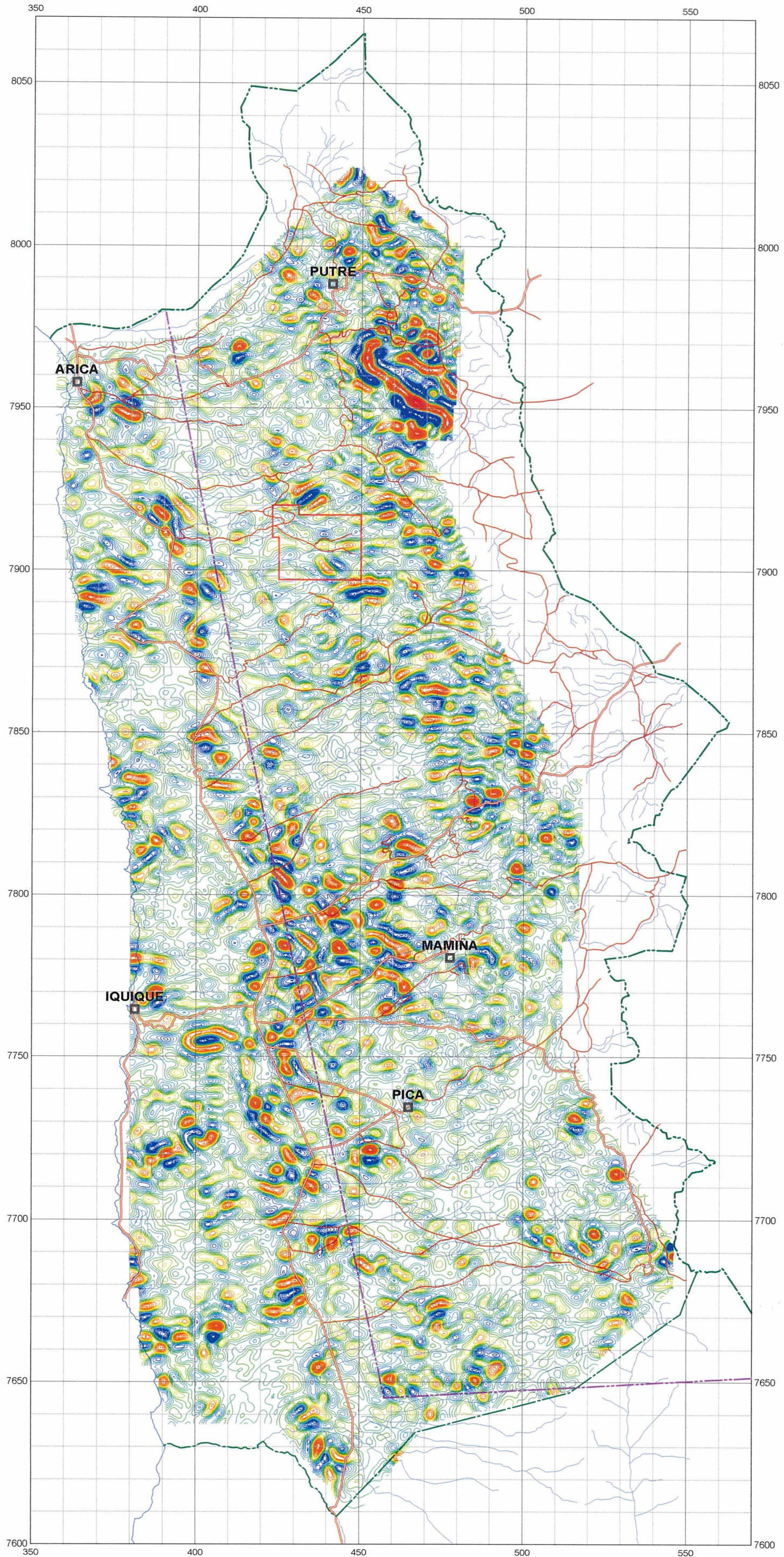


Fig.2-6-4
Short Wavelength
Reduced to the Pole

559

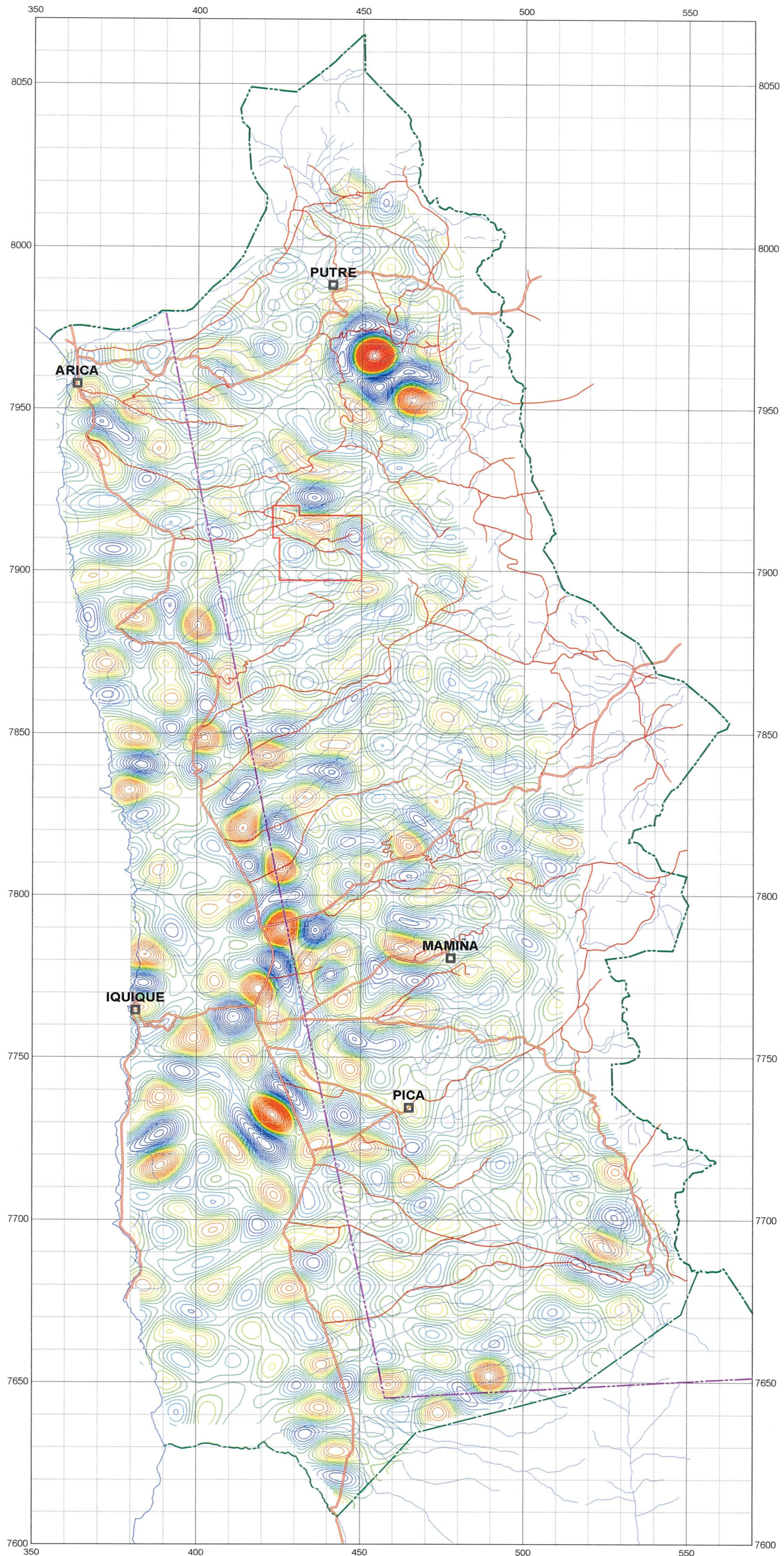
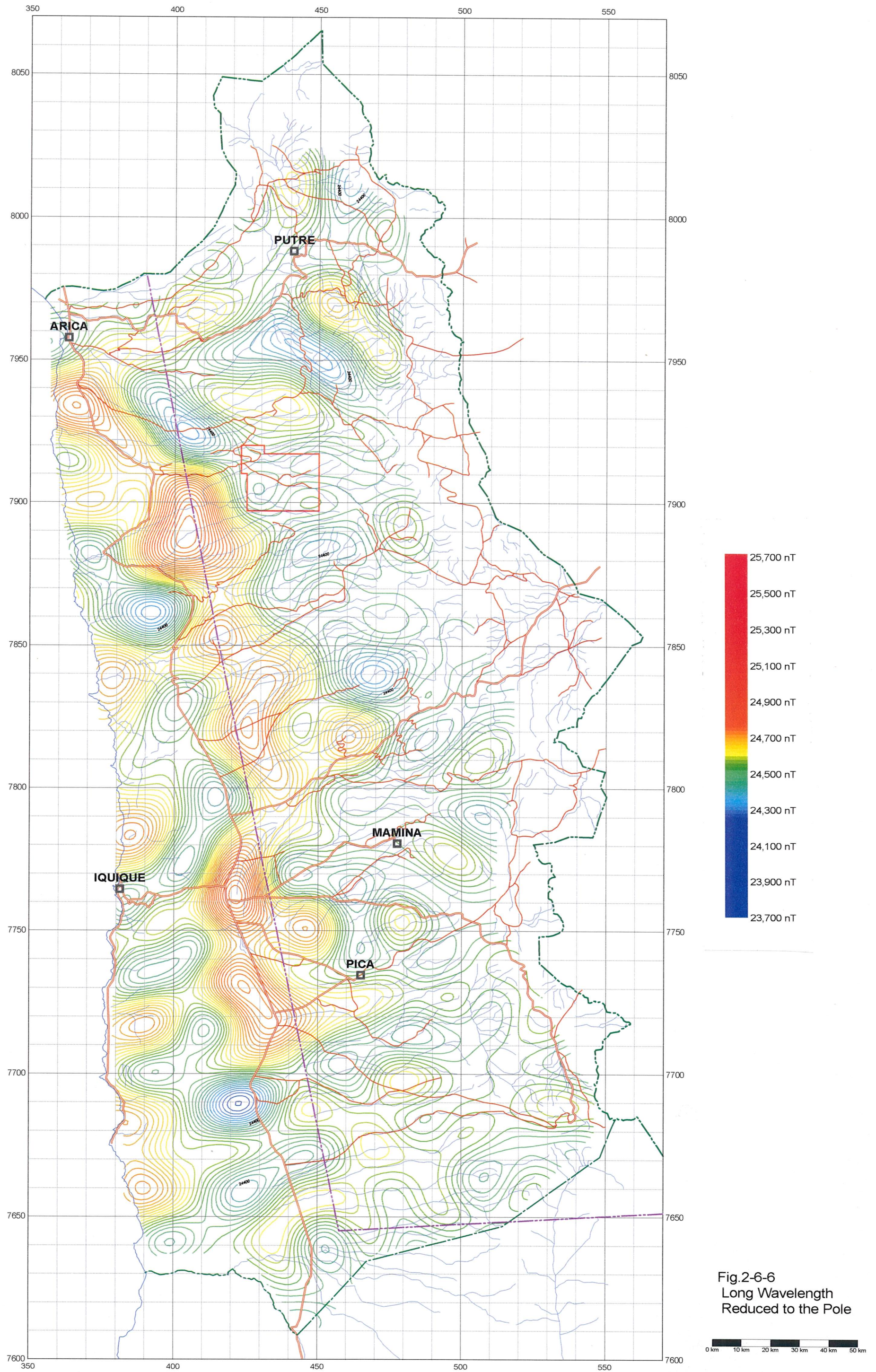


Fig.2-6-5
Medium Wavelength
Reduced to the Pole



— 559 ~ 560 —

561



— 561 ~ 562 —

Fig.2-6-6
Long Wavelength
Reduced to the Pole

0 km 10 km 20 km 30 km 40 km 50 km